

4D RTK: clock solutions and performance

A/Prof Yanming Feng*

Dr Bofeng Li*, **

*Queensland University of Technology

**Tongji University, PR China

Outline

1. Overview of GPS time transfer
2. 3D RTK versus 4D RTK
3. 4D RTK Models and Algorithms
4. Experiments and performance of relative clock solutions
5. Concluding remarks

Overview of GPS Timing applications

Method	Mode	Accuracy	Application
Single point/ Receiver/epoch	One-way mode (OWM)	20-30 ns	Time transfer
Differential GPS Single epoch	Common-view mode (CVM)	5-10 ns	high precision time frequency transfer
Two receivers, long observation time	Melting-pot mode (MPM)	1-3 ns	Remote clock control and steering
Single receiver Continuous data	PPP	0.1 ~0.3ns	Comparison with TWSTFT

3D RTK Vs 4D RTK

- 3D RTK:
 - Clock biases cancelled via double-differencing, only 3 D coordinates to be determined in real time
- 4D RTK:
 - Relative clock biases included in the single-differences, 3D position states and 1D clock bias are determined every epoch (without clock models)
 - Or 1D relative clock is determined if 3D coordinates are given

4D RTK observation models

SD Phase:

$$\begin{bmatrix} L_{1,k} \\ \vdots \\ L_{n,k} \end{bmatrix} = \begin{bmatrix} a_{1,k} \\ \vdots \\ a_{n,k} \end{bmatrix} \delta X_k + c\delta T_k + \lambda \begin{bmatrix} N_1 \\ \vdots \\ N_n \end{bmatrix} + \begin{bmatrix} \varepsilon_{L_{1,k}} \\ \vdots \\ \varepsilon_{L_{n,k}} \end{bmatrix}$$

SD Code:

$$\begin{bmatrix} P_{1,k} \\ \vdots \\ P_{n,k} \end{bmatrix} = \begin{bmatrix} a_{1,k} \\ \vdots \\ a_{n,k} \end{bmatrix} \delta X_k + c\delta T_k + \begin{bmatrix} \varepsilon_{P_{1,k}} \\ \vdots \\ \varepsilon_{P_{n,k}} \end{bmatrix}$$

$$\delta \mathbf{z}_k = \begin{bmatrix} \delta X_k \\ \delta T_k \end{bmatrix} \quad \tilde{\mathbf{B}} = \begin{bmatrix} \lambda \mathbf{1}_n \\ \mathbf{0} \end{bmatrix}$$

$$\tilde{\mathbf{A}}_k = \begin{bmatrix} 1 \\ 1 \end{bmatrix} \otimes [\mathbf{A}_k \quad \mathbf{e}]$$

SD linear model:

$$\mathbf{y}_k = \begin{bmatrix} \tilde{\mathbf{A}}_k & \tilde{\mathbf{B}} \end{bmatrix} \begin{bmatrix} \delta \mathbf{z}_k \\ \mathbf{N} \end{bmatrix} + \boldsymbol{\varepsilon}_{y_k}, \quad \sigma_0^2 \mathbf{Q} = \sigma_0^2 \begin{bmatrix} \mathbf{Q}_L & \mathbf{0} \\ \mathbf{0} & \mathbf{Q}_P \end{bmatrix}$$

4D RTK solutions (1)

Single epoch solution:

$$\begin{bmatrix} \delta \hat{\mathbf{z}}_k \\ \hat{\mathbf{N}} \end{bmatrix} = \begin{bmatrix} \tilde{\mathbf{A}}_k^T \mathbf{Q}^{-1} \tilde{\mathbf{A}}_k & \tilde{\mathbf{A}}_k^T \mathbf{Q}^{-1} \tilde{\mathbf{B}} \\ \tilde{\mathbf{B}}^T \mathbf{Q}^{-1} \tilde{\mathbf{A}}_k & \tilde{\mathbf{B}}^T \mathbf{Q}^{-1} \tilde{\mathbf{B}} \end{bmatrix}^{-1} \begin{bmatrix} \tilde{\mathbf{A}}_k^T \mathbf{Q}^{-1} \mathbf{y}_k \\ \tilde{\mathbf{B}}^T \mathbf{Q}^{-1} \mathbf{y}_k \end{bmatrix}$$

Multiple epoch solution for SD phase ambiguities:

$$\mathbf{R}_k = \mathbf{I} - \tilde{\mathbf{A}}_k \left(\tilde{\mathbf{A}}_k^T \mathbf{Q}^{-1} \tilde{\mathbf{A}}_k \right)^{-1} \tilde{\mathbf{A}}_k^T \mathbf{Q}^{-1}$$

$$\mathbf{Q}_{\hat{\mathbf{N}}} = \left(\tilde{\mathbf{B}}^T \mathbf{Q}^{-1} \sum_{k=1}^m \mathbf{R}_k \tilde{\mathbf{B}} \right)^{-1} \quad \mathbf{w} = \tilde{\mathbf{B}}^T \mathbf{Q}^{-1} \sum_{k=1}^m \mathbf{R}_k \mathbf{y}_k$$

$$\hat{\mathbf{N}} = \mathbf{Q}_{\hat{\mathbf{N}}} \times \mathbf{w}$$

Note: Theoretically, N is non-integers, containing effects of inter-frequency biases

4D RTK solutions (2)

DD ambiguity integer search

$$\mathbf{D} = \begin{bmatrix} -\mathbf{e}_{n-1} & \mathbf{I}_{n-1} \end{bmatrix} \quad \text{Where:} \quad \mathbf{e}_{n-1} = \begin{bmatrix} 1 \\ \vdots \\ 1 \end{bmatrix}$$

DD float ambiguity solution:

$$\Delta \hat{\mathbf{N}} = \mathbf{D} \times \hat{\mathbf{N}} \quad \mathbf{Q}_{\Delta \hat{\mathbf{N}}} = \mathbf{D} \mathbf{Q}_{\hat{\mathbf{N}}} \mathbf{D}^T$$

Integer search:

$$\Delta \tilde{\mathbf{N}} = \arg \min_{\Delta \mathbf{N} \in \mathbb{I}^{n-1}} (\Delta \mathbf{N} - \Delta \hat{\mathbf{N}})^T \mathbf{Q}_{\Delta \hat{\mathbf{N}}}^{-1} (\Delta \mathbf{N} - \Delta \hat{\mathbf{N}})$$

4D RTK solutions (3)

With given coordinates we have:

$$\tilde{\mathbf{A}}_k = \begin{bmatrix} \mathbf{e} \\ \mathbf{e} \end{bmatrix} \quad \delta \mathbf{z}_k = \delta T_k \quad \beta = \sigma_P^2 / \sigma_0^2 \quad \mathbf{e}_n = \begin{bmatrix} 1 \\ \vdots \\ 1 \end{bmatrix}$$

SD phase ambiguity solutions over m epochs:

$$\mathbf{Q}_{\hat{\mathbf{N}}} = \frac{1}{\lambda^2 m} \left(\mathbf{I}_n + \frac{\beta}{n} \mathbf{e} \mathbf{e}^T \right) \quad \mathbf{w} = \lambda \sum_{k=1}^m [\mathbf{L}_k - \mathbf{e} \mathbf{e}^T \left(\frac{\mathbf{L}_k}{n} + \frac{\mathbf{P}_k}{n\beta} \right) / (1 + \frac{1}{\beta})]$$

$$\hat{\mathbf{N}} = \mathbf{Q}_{\hat{\mathbf{N}}} \mathbf{w}$$

where: n is number of satellites
m is number of epochs

The variance estimate:

$$\sigma_0^2 \lambda^2 \mathbf{Q}_{\hat{\mathbf{N}}(i)} \approx \frac{\sigma_P^2}{m \cdot n}$$

4D RTK solutions (4)

The clock solutions (the mth epoch)

$$\delta\bar{z}_m = \frac{1}{n} \left(1 + \frac{1}{\beta}\right)^{-1} e^T \left(L_m + \frac{1}{\beta} P_m - \lambda \hat{N} \right)$$

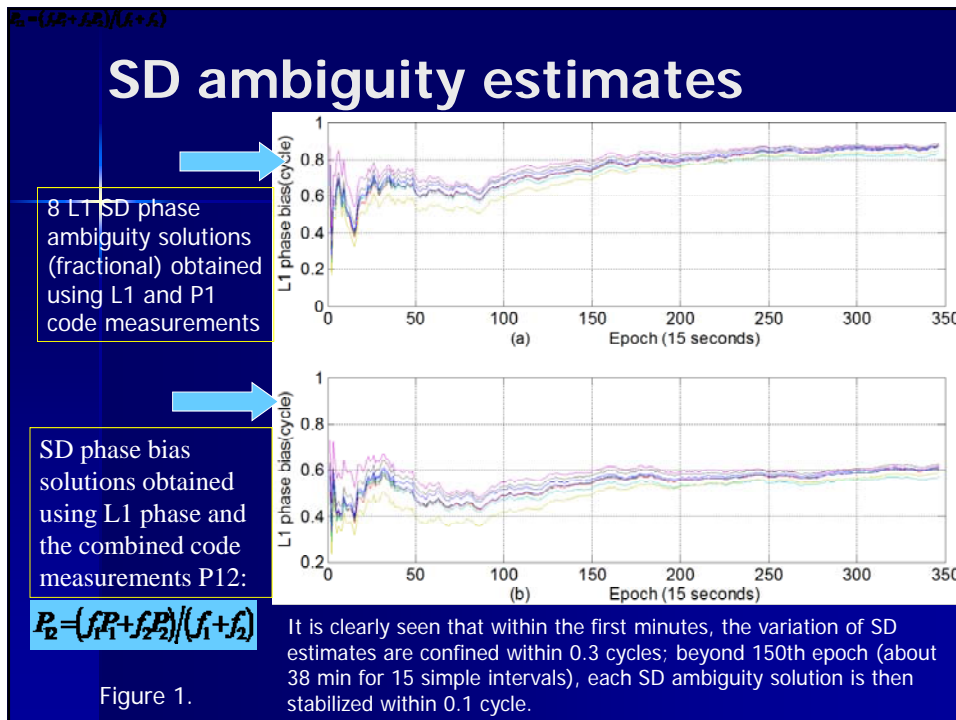
The variance of the clock solution:

$$\sigma_0^2 Q_{\delta\bar{z}} \approx \sigma_0^2 + \frac{\sigma_P^2}{m \Delta t}$$

4. Experimental analysis

Table 1. Experimental Data and Settings for RTK Data Processing

	Data and process settings
Source of data	http://www.ngs.noaa.gov/CORS/cors-data.html , RINEX data: Sites: P474-P478 on 1/1/2007
Observation types	L1, L2, P1,P2
Distance	21km
Cutoff elevation	15 degrees
Number of SVs	8
Data period	00:09:30~01:36:00
Sample rate	15 seconds
Total of epochs	347
Code noise P1,P2 (SD)	0.363m (estimated)
Phase noise L1,L2 (SD)	0.010cm (estimated)



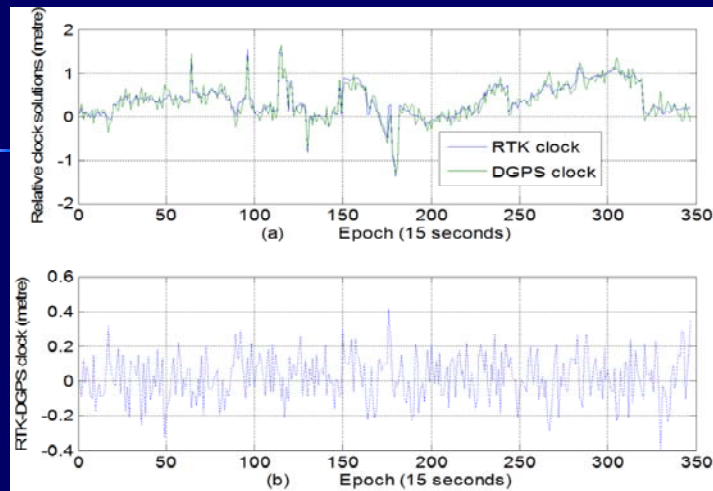


Figure 2: Comparison between RTK and DGPS clock solutions using P12 code measurements in section (a) and differences are shown in section (b).

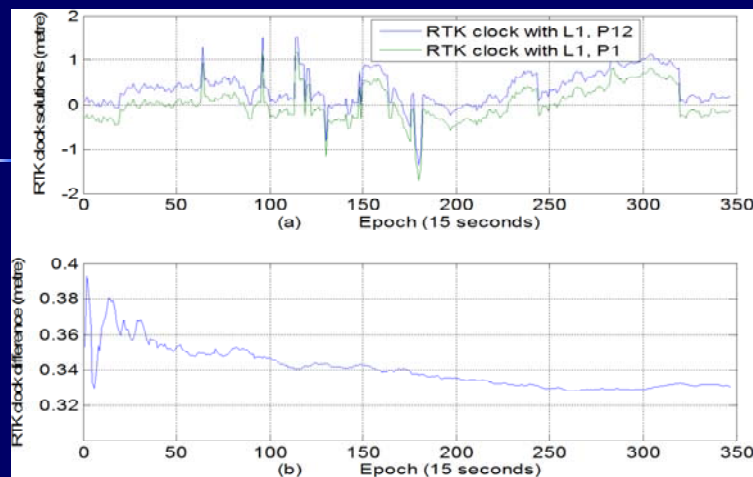


Figure 3. Comparison between two RTK clock solutions obtained with (L1,P1) and (L1,P12) respectively, showing the effects of the receiver-frequency related biases (which should be a constant within hours)

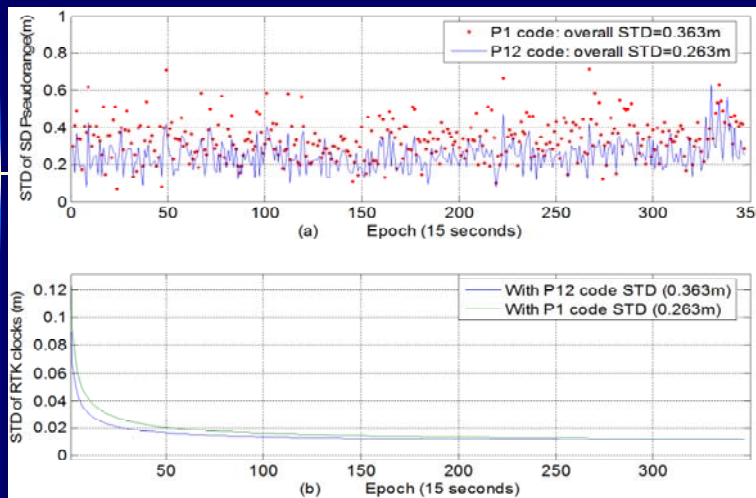


Figure 4 (a) Illustrations of the code STD variations and the overall STD of code P1 and P12 are 0.363m and 0.263 m respectively. The accuracy of the RTK clock solutions reaches the level of 3ns within a few minutes, and converges to 1.5 cm .beyond the 150th epochs.

Conclusions (1)

- Theoretical results:
 - The existing 3D RTK model based on the DD code and phase measurements is a reduced case of the 4D RTK
 - The 3D position states are determined with the DD phase measurements as usual using the existing ILS procedure, the relative clock bias and the SD phase ambiguities are estimated simultaneously epoch by epoch with the SD code and phase observations
 - The constant nature of the SD phase ambiguities allows their estimations to be improved accumulatively; in turn the relative clock solutions are improved from time to time without clock modeling
 - When the user baselines or coordinates are known, the RTK clock solutions can be determined directly from the SD phase and code measurements very easily.

Conclusions (2)

- Experimental results:
 - Within the first few minutes of observations, the SD phase biases fall into the range of 0.3 cycles, achieving a 0.1 to 0.2 ns clock uncertainty.
 - Beyond 150 epochs, the SD phase biases are stabilized within the range of ± 1.5 cm, thus leading the clock biases estimation to the precision and accuracy of 0.05~0.1 ns.
 - The numerical results are consistent with theoretical performance prediction
 - The effects of inter-frequency biases on SD must be removed

Additional Remarks

- The 4D RTK method can potentially provide the most accurate time synchronisations: 0.05-0.1 ns
- The precisely synchronised CORS stations can provide not only provide 3D coordinate datum, but also time datum on a secondly basis
- PPP clocks solutions require satellite clock solutions, which are more complicated
- Comparison with PPP clock solutions is under way

Thank you!

y.feng@qut.edu.au